CES1 is associated with alleviating keloid fibrotic characteristics potentially by modulating JAK/STAT-mediated M2-like macrophage polarization in *in vitro* models

QI JIN[1*], YU HE[1*], JIA QIAO[1], XI FU[1], SHIXING XU[1], HAIHAN SONG[2] and YING CHEN[3]

[1]Department of Craniomaxillofacial Surgery, Plastic Surgery Hospital, Chinese Academy of Medical Sciences and Peking Union Medical College, Beijing 100144, P.R. China; [2]Department of Immunology, DICAT National Biomedical Computation Centre, Vancouver, BC V6B 5A6, Canada; [3]Department of Comprehensive Plastic Surgery, Plastic Surgery Hospital, Chinese Academy of Medical Sciences and Peking Union Medical College, Beijing 100144, P.R. China

Received March 18, 2026; Accepted September 25, 2026

DOI: 10.3892/etm.2026.13347

Abstract. Keloids are characterized by excessive fibrosis driven by interactions between fibroblasts and macrophages. Carboxylesterase 1 (CES1) is associated with fibrosis, but its role in keloid pathogenesis remains unclear. The present study aimed to explore the role of CES1 in keloid fibrosis and its regulation of macrophage-fibroblast interactions. Differential expression analysis was performed on keloid datasets (GSE92566, GSE121618 and GSE158766). KEL FIB cells and M0 macrophages or M2 macrophages were co-cultured. Cellular interactions were evaluated using the Cell Counting Kit-8 assay to assess proliferation, while flow cytometry was used to assess apoptosis. Additionally, fibrosis-related markers (collagen III, collagen I, TGF-β, vimentin, α-smooth muscle actin and fibronectin), M2 macrophage polarization markers (CD206 and CD163) and components of the JAK/STAT signaling pathway were assessed using western blotting, immunofluorescence and reverse transcription-quantitative PCR. Bioinformatics analysis showed that CES1 expression was downregulated in keloid tissues compared with normal skin tissues. Co-culture with M0 macrophages enhanced KEL FIB cell proliferation and reduced apoptosis while upregulating fibrotic markers. Conversely, KEL FIB cells induced M2-like polarization of M0 macrophages, as characterized by the increased expression of CD163 and CD206. CES1 overexpression in KEL FIB cells was associated with reduced phosphorylated STAT5 levels, suggesting a potential modulatory effect on the JAK/STAT signaling pathway, accompanied by decreased expression of fibrotic markers in KEL FIB cells and M2 polarization markers in co-cultured M0 macrophages. CES1 knockdown resulted in the opposite effects, which was mitigated by the STAT5 inhibitor AC-4-130. However, CES1 overexpression did not notably alter fibrotic markers in KEL FIB cells co-cultured with M2 macrophages. The results of the present study suggested a key role for CES1 in modulating keloid fibrosis, possibly by modulating M2 polarization through the JAK/STAT signaling pathway *in vitro*. Targeting CES1 and macrophage-fibroblast interactions may provide a novel research direction and a promising therapeutic strategy for keloid treatment.

Introduction

Keloids result from the excessive proliferation of fibrous tissue after skin injury. These lesions usually appear as thick, hard scars that extend beyond the original wound boundaries and are difficult to heal spontaneously, causing persistent discomfort for patients (1). In one study, the mean age of onset was significantly lower in patients with multiple keloids than in those with solitary keloids (22.65±8.39 vs. 28.19±12.80 years; P=0.006) (2). In addition, ethnicity disparities in keloid susceptibility have been reported, with individuals of black and Asian ethnic backgrounds showing higher odds of keloid occurrence than individuals with white ethnic backgrounds (OR=6.14, 95% CI: 3.75-10.07 and OR=3.70, 95% CI: 2.16-6.34, respectively (3). The most commonly used treatments for keloids include corticosteroid injections, surgical excision, laser therapy and radiotherapy (4,5). However, keloids remain challenging to manage due to their high recurrence rates, which have been reported to range from 33 to 100% depending on treatment modalities (6). The pathophysiology of keloids has been associated with inflammatory mediators, such as IL-8,

Correspondence to: Dr Ying Chen, Department of Comprehensive Plastic Surgery, Plastic Surgery Hospital, Chinese Academy of Medical Sciences and Peking Union Medical College, 33 Badachu Road, Shijingshan, Beijing 100144, P.R. China
E-mail: chenying831119@163.com

*Contributed equally

Key words: carboxylesterase 1, JAK/STAT signaling pathway, keloids, M2 macrophages, fibrosis

TGF-β and IL-6, as well as immune responses involving α-smooth muscle actin (α-SMA) (7). In addition, keloid formation is characterized by the continuous accumulation of extracellular matrix (ECM), primarily driven by fibroblasts via the TGF-β signaling pathway (8). Therefore, research on keloid-related signaling pathways and their regulatory mechanisms is important for the development of effective treatment strategies.

Macrophages are immune cells integral to maintaining immune homeostasis, tissue repair and the inflammatory response (9). Macrophages regulate these processes by producing various cytokines, including IL-6, IL-1 and TNF-α. Depending on the microenvironment, macrophages can differentiate into M1 (classically activated) or M2 (alternatively activated) phenotypes (10). M2 macrophages are typically associated with fibrosis and the healing process, and they have been shown to promote scar formation. Several studies have highlighted the notable function of macrophages in the formation and progression of keloids. Seoudy *et al* (11) demonstrated that keloid tissues exhibit low levels of M1 macrophages, while M2 macrophages are notably elevated. Furthermore, Dirand *et al* (12) found that M2 macrophages enhance the fibrotic characteristics of keloid fibroblasts, whereas M1 macrophages exhibit antifibrotic properties. This suggests that the M1/M2 macrophage subtypes have distinct effects on the fibrotic process in keloids, and restoring the balance between these two populations may represent an effective therapeutic strategy. Given these insights, the present study investigated the impact of macrophages on fibroblasts and further elucidated the specific mechanisms underlying keloid formation.

The JAK/STAT signaling pathway is essential for regulating cellular processes such as differentiation, survival, proliferation and immune responses (13). Abnormal activation of the JAK/STAT pathway has been associated with several diseases, including cancer (14). In fibrotic diseases, sustained activation of the JAK/STAT signaling pathway leads to excessive ECM deposition and tissue remodeling, thereby exacerbating disease progression (15). Clinical research has shown that JAK/STAT inhibitors effectively hinder keloid progression by reducing collagen production, cellular migration and proliferation, as well as by inducing apoptosis and halting the cell cycle (16). Furthermore, research has shown that fibroblasts activated by WNT5A secrete IL-6, which subsequently activates the JAK/STAT signaling pathway, promoting epithelial-mesenchymal transition in neighboring keratinocytes (17).

Recent studies have emphasized the key function of macrophages in the fibrotic response, particularly the influence of M2 macrophages, which have been shown to promote fibrosis through cytokine release and interaction with fibroblasts (18,19). The JAK/STAT signaling pathway may help modulate these fibrotic processes, and abnormal activation has been associated with keloid development. Carboxylesterase 1 (CES1) is a member of the serine hydrolase superfamily that catalyzes ester hydrolysis and is increasingly investigated for its role in drug metabolism (20). In addition to its established role in xenobiotic metabolism, CES1 is involved in lipid metabolism and has been associated with metabolic disorders and liver fibrosis (21). The present study explored the potential association and investigated the role of CES1 and the JAK/STAT signaling pathway in fibrotic processes in keloid fibroblasts. By exploring the functional relationships among CES1, macrophage polarization and fibroblast behavior, the obtained findings may offer insights into potential mechanisms underlying keloid formation, and may provide preliminary clues for new avenues for therapeutic intervention to address the challenges posed by keloid treatment.

Materials and methods

Retrieval of keloid-related datasets. In the present study, gene expression profiles associated with keloids were analyzed using data from Gene Expression Omnibus (https://www.ncbi.nlm.nih.gov/geo/). A total of three relevant datasets (GSE92566, GSE121618 and GSE158766) were selected (22,23). The GSE92566 dataset consists of four keloid skin samples (case group) and three adjacent non-lesional skin samples (control group), enabling comparison of gene expression between keloid-affected and healthy tissues. The GSE121618 dataset contains five endothelial cell samples isolated from keloid tissue (case group) and six samples derived from normal skin (control group), providing a basis for investigating differences in endothelial cell behavior associated with keloid pathogenesis. Finally, the GSE158766 dataset comprises six samples of proliferative scar cells (case group) and three normal skin cell samples (control group), enabling analysis of gene expression alterations associated with scar formation.

Expression analysis of overlapping genes in three keloid-related datasets. Differential gene expression analysis was conducted on the keloid-associated datasets (GSE92566, GSE121618 and GSE158766) utilizing the 'limma' package in R software (version 3.42.2; https://bioconductor.org/packages/limma/). Briefly, background correction and quantile normalization were performed to standardize gene expression profiles across datasets. To minimize technical variation and reduce inter-dataset heterogeneity, the datasets were merged and subjected to batch-effect correction before downstream analysis. Differentially expressed genes (DEGs) were identified using fold-change (FC)-based screening, with FC>1.3 defining upregulated genes and FC<0.7 defining downregulated genes, combined with a nominal $P<0.05$. Given the limited sample sizes of the original datasets, FC-based screening was prioritized over strict multiple-testing correction to reduce the risk of excluding biologically relevant genes due to low statistical power. Experimental approaches subsequently validated the candidate genes. Following the identification of DEGs, overlapping upregulated and downregulated DEGs among the three datasets were identified using the Venn diagram online tool (https://bioinformatics.psb.ugent.be/webtools/Venn/). The expression patterns of the overlapping genes in keloid and normal control samples were subsequently analyzed and visualized using the Sangerbox platform (version 3.0; http://vip.sangerbox.com/home.html).

Cell lines and culture. For cellular experiments, the human keloid fibroblast cell line KEL FIB (cat. no. CRL-1762) was purchased from the American Type Culture Collection, and human monocytic THP-1 cells were sourced from The Type Culture Collection Cell Bank of the Chinese Academy

of Sciences Committee. Both cell lines were subjected to short tandem repeat profiling identification and mycoplasma detection by the suppliers and were confirmed free of cross-contamination. KEL FIB cells were cultured in DMEM (Gibco; Thermo Fisher Scientific, Inc.) with 10% FBS (Gibco; Thermo Fisher Scientific, Inc.) and 1% penicillin-streptomycin. THP-1 cells were maintained in RPMI-1640 medium (Gibco; Thermo Fisher Scientific, Inc.) supplemented with 1% penicillin-streptomycin and 10% FBS. All cell cultures were incubated in a 5% CO_2 atmosphere at 37˚C.

Macrophage differentiation and co-culture with KEL FIB cells. Following the protocol established by Hickman *et al* (24), THP-1 cells were treated with 40 ng/ml macrophage colony-stimulating factor (cat. no. P5313; Beyotime Biotechnology) for 48 h at 37˚C to induce their differentiation into M0 macrophages. To confirm successful differentiation, cells were examined for morphological changes under an inverted light microscope. Differentiated M0 macrophages exhibited characteristic adherent morphology with elongated, spindle-shaped or star-like appearance, in contrast to the round, floating morphology of undifferentiated THP-1 monocytes. To further differentiate M0 macrophages into M2 macrophages, 20 ng/ml IL-4 (cat. no. P5129; Beyotime Biotechnology) was added to the culture medium for 24 h at 37˚C. For the indirect co-culture assay, KEL FIB cells were first seeded into the lower chamber of 6-well Transwell inserts with 0.4-μm pores at a density of $1x10^5$ cells per well and cultured overnight to allow cell attachment. Subsequently, differentiated M0 or M2 macrophages were seeded in the upper chamber at $1x10^5$ cells per well in complete RPMI-1640 medium containing 10% FBS and 1% penicillin-streptomycin. KEL FIB cells in the lower chamber were maintained in DMEM supplemented with 10% FBS and 1% penicillin-streptomycin. The two cell populations were physically separated by the Transwell membrane, which allowed the exchange of soluble factors. The indirect co-culture was maintained for 48 h at 37˚C in a humidified incubator containing 5% CO_2.

Cell treatments. For TGF-β treatment, KEL FIB cells were incubated at 37˚C for 24 h in complete growth medium supplemented with 10% FBS and 1% penicillin-streptomycin containing 5 ng/ml TGF-β (Beyotime Biotechnology). To inhibit phosphorylated (p)STAT5 signaling, DMSO was employed to dissolve the STAT5 inhibitor AC-4-130 (MedChemExpress), which was then added at a final concentration of 5 μM to the KEL FIB cell culture medium containing 10% FBS and 1% penicillin-streptomycin, and the cells were incubated at 37˚C for 24 h. Control groups were treated with an equivalent volume of DMSO to ensure consistency across experimental conditions.

Cell transfection. KEL FIB cells were cultured at a seeding density of $2x10^5$ cells per well in 24-well plates. Cells were incubated overnight in complete growth medium to achieve 70-80% confluence. Transfections were conducted using Lipofectamine® 2000 reagent (Invitrogen; Thermo Fisher Scientific, Inc.) according to the manufacturer's instructions. KEL FIB cells were transfected with a pcDNA3.1-based plasmid for CES1 overexpression (over-CES1) or the control vector (vector) (Shanghai GenePharma Co., Ltd.). The plasmid was used at 0.5 μg per well. Additionally, small interfering RNA (siRNA) targeting CES1 (si-CES1; sense, 5'-CCUGCUG ACUUGACCAAGAAA-3'; and antisense, 5'-UUUCUUGGU CAAGUCAGGCAGG-3') or negative control siRNA (si-NC; sense, 5'-UUCUCCGAACGUGUCACGUTT-3'; and antisense, 5'-ACGUGACACGUUCGGAGAATT-3') (Shanghai GenePharma Co., Ltd.) was transfected into separate groups of KEL FIB cells at a final concentration of 50 nM. Transfection was performed at 37˚C for 6 h, after which the medium was replaced with fresh complete growth medium. For co-culture experiments, KEL FIB + M0 macrophages and KEL FIB + M2 macrophages were co-cultured after transfecting KEL FIB cells with either over-CES1 or vector plasmids. All transfection procedures adhered to standardized protocols. Cells were harvested for subsequent analyses after 48 h of transfection.

Cell Counting Kit-8 (CCK-8) assay. Cell proliferation was assessed using the CCK-8 assay (cat. no. CK04; Dojindo Laboratories, Inc.). For co-culture experiments, KEL FIB cells and M0 macrophages were first co-cultured using the 6-well Transwell system at $1x10^5$ cells per well under the conditions aforementioned. Following co-culture, the indicated cells were collected and re-seeded into 96-well plates for the CCK-8 assay. Following the aforementioned treatments, CCK-8 reagent was added to each well, and the cells were incubated for 2 h at 37˚C. Absorbance was measured at 450 nm using a microplate reader (Thermo Fisher Scientific, Inc.) on days 1, 2, 3 and 4.

Flow cytometry analysis. Flow cytometry was used to assess apoptosis in KEL FIB cells and M0 macrophages under the indicated experimental conditions. KEL FIB cells cultured alone or treated with TGF-β were seeded at a density of $1x10^5$ cells per well in 24-well plates and cultured for 24 h before treatment. KEL FIB cells co-cultured with M0 macrophages were cultured using the 6-well Transwell system aforementioned. After the indicated treatment or 48 h of co-culture, KEL FIB cells were collected for apoptosis analysis. For M0 macrophage experiments, M0 macrophages were cultured alone or co-cultured with KEL FIB cells using the same Transwell system, and M0 macrophages were collected after 48 h for apoptosis analysis. Cells were dissociated using trypsin-EDTA, washed with PBS and resuspended in binding buffer provided with the Annexin V-FITC Early Apoptosis Detection Kit (cat. no. 6592; Cell Signaling Technology, Inc.). For apoptosis analysis, the cell suspension was incubated at room temperature in the dark for 15 min after adding 5 μl annexin V-FITC solution and 5 μl PI. The stained cells were analyzed with a CyFlow Space flow cytometer (Sysmex Partec GmbH), and the data were processed using FlowJo software (version 10.6.1; FlowJo, LLC; Waters Biosciences).

Reverse transcription-quantitative PCR (RT-qPCR). Total RNA was extracted from KEL FIB cells, M0 macrophages or M2 macrophages with RNAiso Plus (cat. no. 9108; Takara Biotechnology Co., Ltd.) as per the manufacturer's instructions. cDNA synthesis was conducted using the PrimeScript RT Reagent Kit (Takara Bio, Inc.) according to the manufacturer's instructions. The SYBR Green PCR Master Mix (Vazyme

Biotech Co., Ltd.) was then used to perform RT-qPCR on the resulting cDNA using a StepOnePlus Real-Time PCR System (Applied Biosystems; Thermo Fisher Scientific, Ltd.). The amplification conditions were as follows: Initial denaturation at 95˚C for 30 sec, followed by 40 cycles of denaturation at 95˚C for 5 sec and annealing/extension at 60˚C for 30 sec. A melting-curve analysis was performed at the end of the amplification to verify the specificity of the products. The primer sequences used for amplification were as follows: CES1 forward, 5'-GATGTGGCTCCGTGCCTTTA-3' and reverse, 5'-TTCCCAGGAAAATGGCCACA-3'; CD206 forward, 5'-TTCCTTTGGACGGATGGACG-3' and reverse, 5'-CCTCGTTTACTGTCGCAGGT-3'; CD163 forward, 5'-GAAGACAGAGACAGCGGCTT-3' and reverse, 5'-GGTATCTTAAAGGCTCACTGGGT-3'. The forward and reverse primers for GAPDH, which was used as a reference internal control, were as follows: GAPDH forward, 5'-ATGAATGGGCAGCCGTTAGG-3' and reverse, 5'-CGCCCAATACGACCAAATCA-3'. The $2^{-\Delta\Delta Cq}$ method was used to determine the relative expression of target genes (25).

Western blot (WB) analysis. Protein lysates from KEL FIB cells and macrophages under the indicated experimental conditions were prepared using RIPA lysis buffer (Thermo Fisher Scientific, Ltd.), supplemented with protease and phosphatase inhibitors. Protein concentration was determined using the BCA Protein Assay Kit (Beyotime Biotechnology). Proteins in equal quantities (30 μg per lane) were separated with 10% SDS-PAGE and then transferred to PVDF membranes (Merck KGaA). The membranes were blocked with 5% non-fat milk in TBST containing 0.1% Tween-20 for 1 h at room temperature. For blots displaying a target protein together with GAPDH, the corresponding primary antibodies were incubated simultaneously on the same PVDF membrane, and the resulting bands were distinguished according to their expected molecular weights. The membranes were incubated with the corresponding primary antibodies for 1 h at room temperature. The following primary antibodies were used to probe the membranes: Collagen III (1:1,000; cat. no. ab184993), collagen I (1:1,000; cat. no. ab138492), TGF-β (1:1,000; cat. no. ab215715), vimentin (1:1,000; cat. no. ab92547), fibronectin (1:1,000; cat. no. ab2413), CES1 (1:10,000; cat. no. ab53008), CD206 (1:1,000; cat. no. ab64693), CD163 (1:1,000; cat. no. ab182422) and GAPDH (1:10,000; cat. no. ab181602), all purchased from Abcam. The α-SMA antibody (1:500; cat. no. A5228) was obtained from Sigma-Aldrich (Merck KGaA). STAT5 (1:1,000; cat. no. 94205) and pSTAT5 (1:1,000; cat. no. 9359) antibodies were acquired from Cell Signaling Technology, Inc. Following incubation with primary antibodies, the membranes were washed with TBST and incubated for 1 h at room temperature with HRP-conjugated goat anti-rabbit IgG H&L (1:5,000; cat. no. ab6721; Abcam) or HRP-conjugated goat anti-mouse IgG H&L (1:5,000; cat. no. ab97023; Abcam). Protein bands were visualized using ECL reagent (Beyotime Biotechnology) and semi-quantified with ImageJ software (version 1.8.0; National Institutes of Health).

Immunofluorescence analysis. Immunofluorescence staining was performed to evaluate the localization and expression of α-SMA in KEL FIB cells, KEL FIB cells co-cultured with M0 macrophages and KEL FIB cells exposed to 5 ng/ml TGF-β. After fixation for 30 min at room temperature with 4% paraformaldehyde (Wuhan Servicebio Technology Co., Ltd.), the cells were permeabilized for 15 min using 0.1% Triton X-100 (Beijing Solarbio Science & Technology Co., Ltd.) at room temperature. To prevent non-specific binding, the cells were treated with 5% BSA (Gibco; Thermo Fisher Scientific, Ltd.) for 1 h at room temperature following three rounds of washing with PBS. The cells were then incubated with a primary antibody against α-SMA (1:50; cat. no. AG0101; Beyotime Biotechnology) at 4˚C overnight. After washing with PBS, cells were treated with Alexa Fluor 594-conjugated AffiniPure Goat Anti-Rabbit IgG (H+L) secondary antibody (1:500; cat. no. 111-585-003; Jackson ImmunoResearch Laboratories, Inc.) at room temperature for 1 h in the dark. Cell nuclei were counterstained with DAPI (5 μg/ml; cat. no. C0066; Beijing Solarbio Science & Technology Co., Ltd.) for 10 min at room temperature. A fluorescence microscope (Olympus Corporation) was used to obtain fluorescence images, and the expression and localization of α-SMA were analyzed using ImageJ software (version 1.8.0; National Institutes of Health, USA).

Statistical analysis. The R software (version 4.3.2; R Foundation for Statistical Computing) was used for statistical analysis. Three independent biological replicates were performed, each with three technical replicates, and the mean of the technical replicates was used for analysis. Data are presented as the mean ± SD or as box-and-whisker plots. For comparisons between two experimental groups, an unpaired Student's t-test was used. The Mann-Whitney U test was used for non-parametric comparisons between two groups. One-way ANOVA was used to assess significant differences among groups, and Tukey's post hoc test was conducted for pairwise comparisons. Two-way ANOVA followed by Tukey's post hoc test was conducted for analyses involving multiple factors. Box-and-whisker plots are presented as the median and interquartile range. $P<0.05$ was considered to indicate a statistically significant difference.

Results

Identification of DEGs and the hub gene CES1 in keloid datasets. In the present study, differential expression analysis was conducted on keloid-related datasets, GSE92566, GSE121618 and GSE158766, using the R 'limma' package. As illustrated in Fig. 1A, analysis of the GSE92566 dataset revealed 1,140 upregulated DEGs and 2,246 downregulated DEGs in the case group relative to the control group. Similarly, the GSE121618 dataset exhibited 1,038 downregulated and 1,702 upregulated DEGs (Fig. 1B). Furthermore, the GSE158766 dataset showed 207 upregulated DEGs and 86 downregulated DEGs in the case group relative to the control group (Fig. 1C). Subsequent analysis of the upregulated DEGs across the three datasets identified one overlapping gene (Fig. 1D). Additionally, two overlapping genes were found among the downregulated DEGs across the three datasets (Fig. 1E). Finally, expression analysis of the overlapping genes CES1, procollagen-lysine, 2-oxoglutarate 5-dioxygenase 3 (PLOD3) and semaphorin 3G (SEMA3G) in the control and

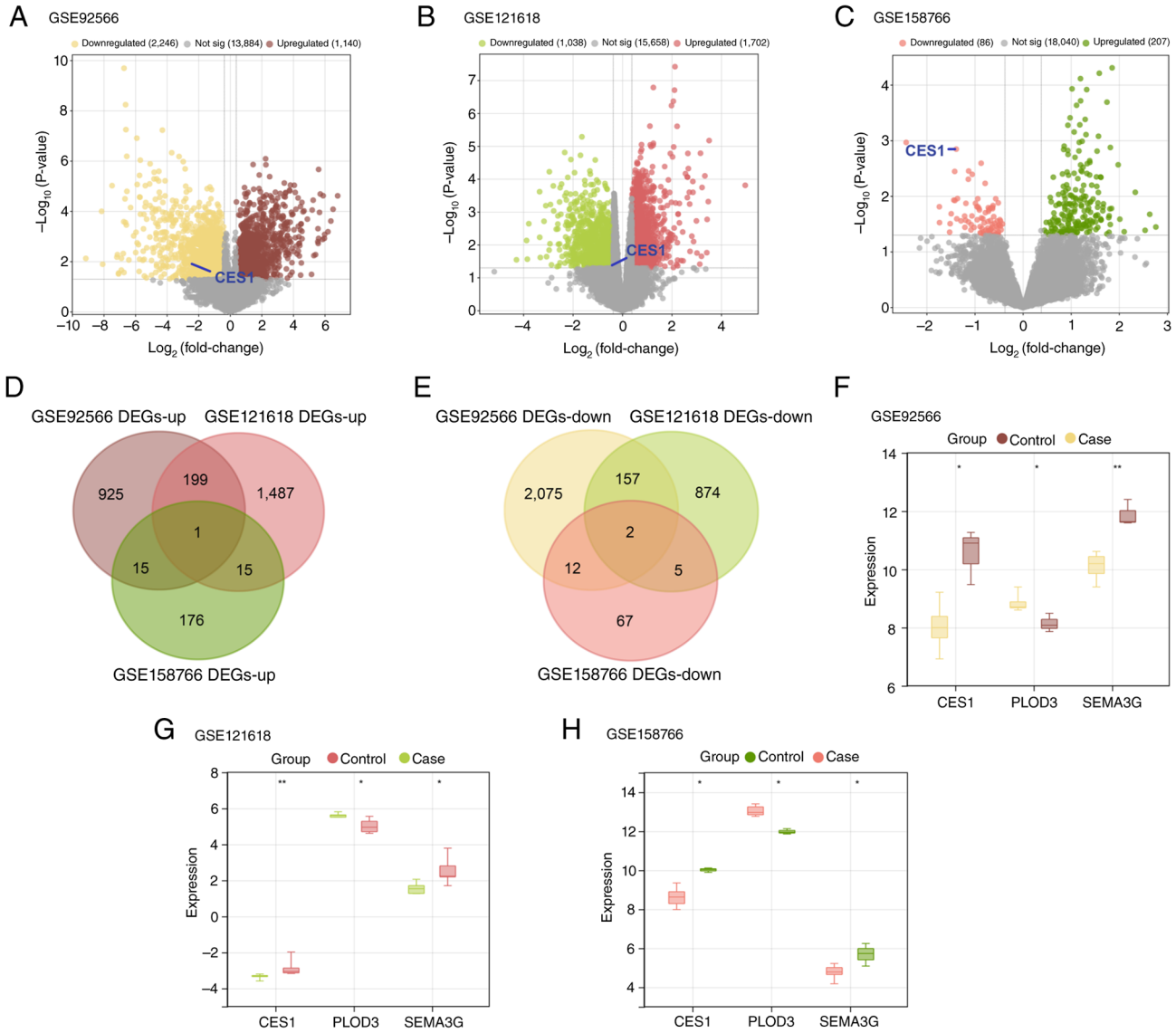


Figure 1. Screening of DEGs and expression verification of key genes in keloid datasets. (A) Volcano plot displaying DEGs in the GSE92566 dataset. Brown dots indicate upregulated DEGs, while yellow dots indicate downregulated DEGs. (B) Volcano plot for DEGs in the GSE121618 dataset. Red dots indicate upregulated DEGs, while green dots indicate downregulated DEGs. (C) Volcano plot for DEGs in the GSE158766 dataset. Green dots indicate upregulated DEGs, while red dots indicate downregulated DEGs. (D) Venn diagram illustrating overlapping upregulated DEGs among the three datasets (GSE92566, GSE121618 and GSE158766). (E) Venn diagram showing overlapping downregulated DEGs across the three datasets (GSE92566, GSE121618 and GSE158766). Expression levels of the overlapping genes (CES1, PLOD3 and SEMA3G) in the control and case groups across the (F) GSE92566, (G) GSE121618 and (H) GSE158766 datasets. Group comparisons were performed using the Mann-Whitney U test. *P<0.05 and **P<0.01 vs. control. DEG, differentially expressed gene; CES1, carboxylesterase 1; PLOD3, procollagen-lysine, 2-oxoglutarate 5-dioxygenase 3, SEMA3G, semaphorin 3G; not sig, not significant.

case groups across the three datasets indicated that CES1 and SEMA3G were downregulated in the case group, whereas PLOD3 was upregulated (Fig. 1F-H). Previous studies have demonstrated that CES1 is linked to pathways associated with lipid metabolism, inflammation and tissue remodeling (26,27). These processes are highly relevant to keloid pathogenesis, suggesting that CES1 may regulate keloid development. In addition, the consistent dysregulation of CES1 across multiple datasets further supports its potential relevance in disease progression. Therefore, CES1 was selected as a hub gene for subsequent analysis.

Reciprocal pro-survival interaction between M0 macrophages and KEL FIB. TGF-β is a key driver of fibroblast-mediated fibrosis and scar formation, leading to abnormal tissue repair and fibrotic processes by activating fibroblasts, promoting ECM synthesis and inducing inflammation (28). In the present study, the proliferation of KEL FIB cells under different conditions was evaluated using the CCK-8 assay (Fig. 2A). Compared with KEL FIB cells cultured alone, co-culture with M0 macrophages notably promoted the proliferation of KEL FIB cells from day 3. In addition, treatment with 5 ng/ml TGF-β also promoted KEL FIB cell proliferation. The apoptosis rate of KEL FIB cells under different conditions was examined through flow cytometry (Fig. 2B). A significant reduction in the apoptosis rate was observed in KEL FIB cells co-cultured with M0 macrophages compared with those cultured alone. Treatment with 5 ng/ml TGF-β also significantly reduced apoptosis in KEL FIB cells compared with cells cultured alone. To determine whether this interaction is reciprocal, the effects

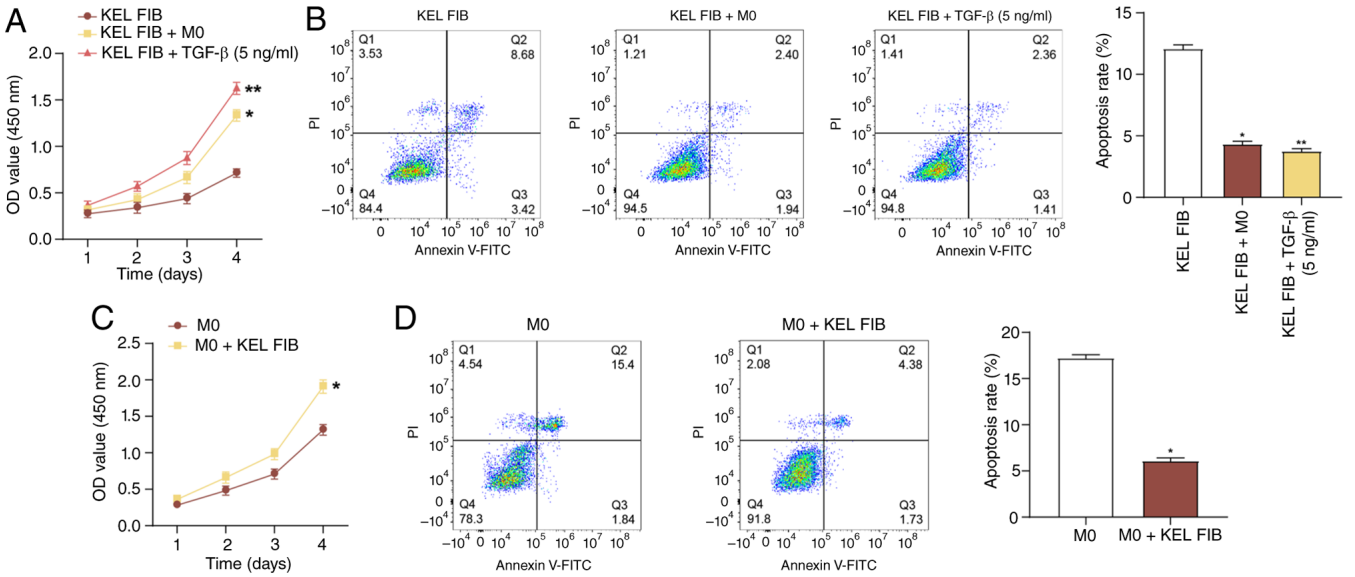


Figure 2. Bidirectional crosstalk between M0 macrophages and KEL FIB cells enhances proliferation and reduces apoptosis. (A) CCK-8 assay results showing the proliferative response of KEL FIB cells in co-culture with M0 macrophages or treated with TGF-β (5 ng/ml). *P<0.05 and **P<0.01 vs. KEL FIB group. Statistical analysis was performed using two-way ANOVA followed by Tukey's post hoc test. (B) Cells were stained with annexin V-FITC and PI to assess apoptosis in different treatment conditions [KEL FIB, KEL FIB + M0 or KEL FIB + TGF-β (5 ng/ml)]. The percentage of apoptotic cells is indicated for each condition (Q2 + Q3 quadrants). Statistical analysis was performed using one-way ANOVA followed by Tukey's post hoc test. *P<0.05 and **P<0.01 vs. KEL FIB group. (C) CCK-8 assay showing the proliferation of M0 macrophages cultured alone or co-cultured with KEL FIB cells over 4 days. *P<0.05 vs. M0 group. Statistical analysis was performed using two-way ANOVA followed by Tukey's post hoc test. (D) Representative annexin V-FITC and PI flow cytometry plots and quantitative analysis of apoptosis in M0 macrophages cultured alone or co-cultured with KEL FIB cells. Statistical analysis was performed using unpaired Student's t-test. *P<0.05 vs. M0 group. Data are presented as the mean ± SD (n=3). CCK-8, Cell Counting Kit-8; OD, optical density.

of KEL FIB cells on the proliferative capacity and apoptotic status of M0 macrophages were further assessed. The CCK-8 assay showed that co-culture with KEL FIB cells significantly increased the proliferation of M0 macrophage compared with that of M0 macrophages cultured alone (Fig. 2C). Flow cytometry analysis showed that co-culture with KEL FIB cells significantly reduced the apoptosis of M0 macrophages compared with that of cells cultured alone, indicating that KEL FIB cells have an anti-apoptotic protective effect on M0 macrophages (Fig. 2D). Collectively, the present findings demonstrated a reciprocal pro-proliferative and anti-apoptotic interaction between M0 macrophages and KEL FIB cells, suggesting a feed-forward cellular circuit that may facilitate fibrotic remodeling.

M0 macrophages promote upregulation of fibrosis markers in KEL FIB cells. To further clarify the impact of M0 macrophages on scar fibroblast-mediated fibrosis, WB analysis was conducted to assess the levels of fibrosis-associated markers (collagen III, collagen I, TGF-β, vimentin, α-SMA and fibronectin) in M0 macrophage and KEL FIB cell co-cultures as well as TGF-β-treated KEL FIB cells. The results indicated that co-culture with M0 macrophages significantly elevated fibrosis marker levels compared with those in the KEL FIB cell-only group, a trend similarly observed with TGF-β treatment (Fig. 3A and B). Immunofluorescence analysis further supported these findings, showing a marked increase in α-SMA fluorescence intensity in KEL FIB cells co-cultured with M0 macrophages, indicating upregulation of this fibrosis marker. TGF-β-treated KEL FIB cells also exhibited a notable increase in α-SMA fluorescence intensity (Fig. 3C). These results suggest that macrophages can induce fibrotic transformation in KEL FIB cells.

KEL FIB cells induce M2-like polarization of M0 macrophages. CD206 and CD163 are hallmark markers of M2 macrophages (29). Whether KEL FIB cells cause M0 macrophages to become M2-polarized was evaluated by measuring the levels of M2 macrophage markers (CD206 and CD163). RT-qPCR experimental results showed that the expression levels of CD206 and CD163 were upregulated in M0 macrophages following co-culture with KEL FIB cells (Fig. 4A). Subsequent WB analysis confirmed that CD206 and CD163 protein levels were increased in co-cultured M0 macrophages compared with those in the M0 macrophage group alone (Fig. 4B and C). These findings suggest that keloid fibroblasts drive M2-like polarization in macrophages.

Regulation of CES1 expression in KEL FIB cells by M0 macrophages and TGF-β. To investigate the role of CES1 in keloid fibroblasts, RT-qPCR experiments were conducted to confirm that the mRNA expression of CES1 in KEL FIB cells was markedly reduced when co-cultured with M0 macrophages or treated with 5 ng/ml TGF-β compared with that in KEL FIB cells cultured alone (Fig. 5A). These results were also confirmed at the protein level through WB experiments, showing a decrease in CES1 protein in KEL FIB cells after co-culture with M0 macrophages or application of 5 ng/ml TGF-β (Fig. 5B and C). To further explore the functional role of CES1, the efficiency of CES1 knockdown and overexpression was verified by transfecting KEL FIB cells with CES1-targeting molecules followed by RT-qPCR and WB

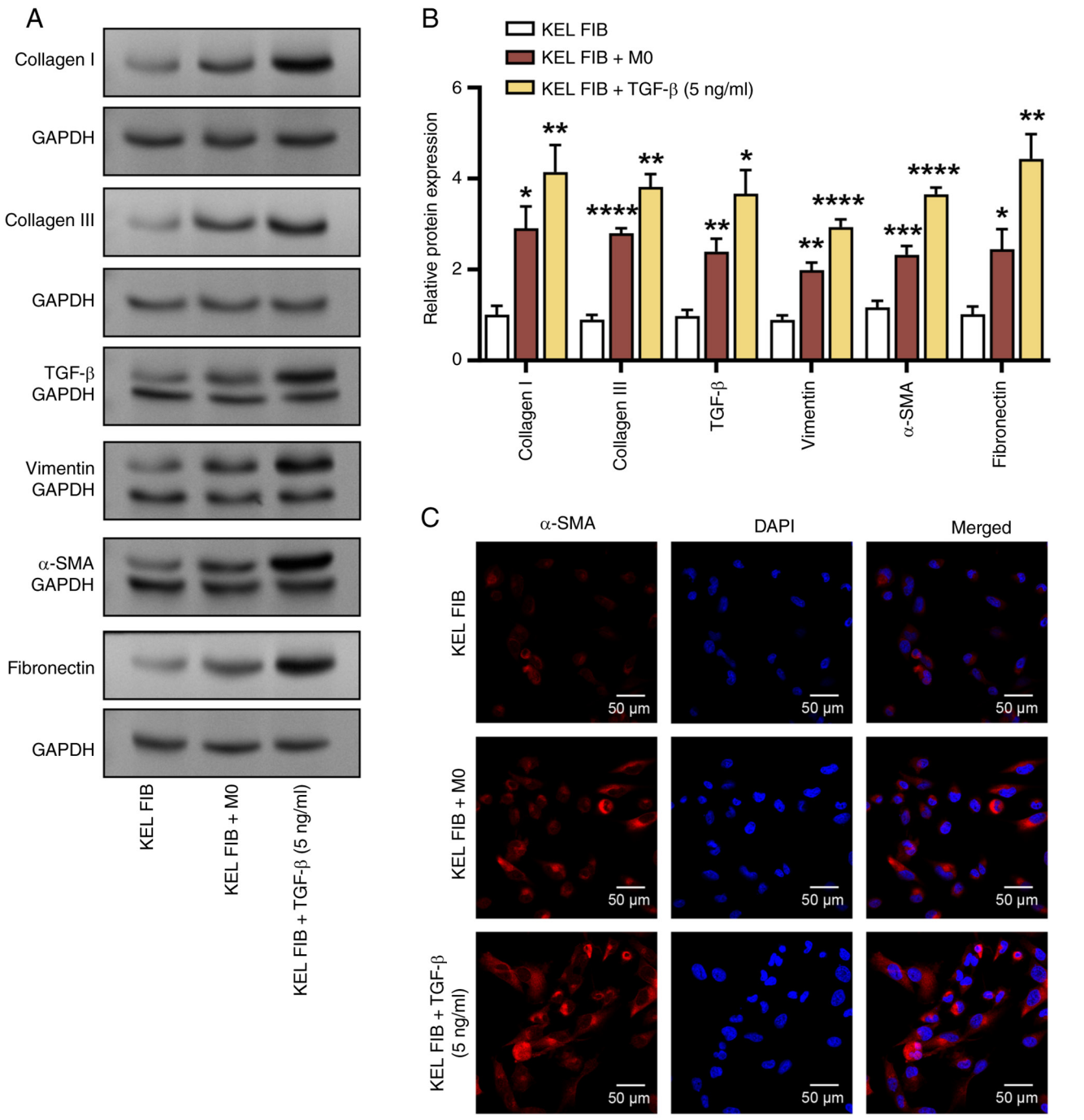


Figure 3. Effects of M0 macrophages and TGF-β on the expression of fibrosis-related markers in KEL FIB cells. (A) WB analysis depicting the levels of fibrosis markers (collagen I, collagen III, TGF-β, vimentin, α-SMA and fibronectin) in KEL FIB cells following co-culture with M0 macrophages or treatment with TGF-β (5 ng/ml). (B) Semi-quantitative analysis of fibrosis marker expression in KEL FIB cells, derived from WB data. Statistical analysis was performed using one-way ANOVA followed by Tukey's post hoc test. (C) Immunofluorescence staining showing α-SMA expression (red) and cell nuclei counterstained with DAPI (blue) in KEL FIB cells under the indicated conditions. Merged images demonstrate the expression and localization of α-SMA in KEL FIB cells co-cultured with M0 macrophages or treated with TGF-β (5 ng/ml). Data are presented as the mean ± SD (n=3). Scale bar, 50 μm. *P<0.05, **P<0.01, ***P<0.001 and ****P<0.0001 vs. KEL FIB group. WB, western blot; α-SMA, α-smooth muscle actin.

analyses, confirming effective regulation of CES1 levels (Fig. 5D-G).

Overexpression of CES1 is associated with reduced JAK/STAT signaling and decreased fibrosis markers in keloid fibroblasts. To explore the impact of CES1 on the JAK/STAT signaling cascade and fibrosis in KEL FIB under co-culture conditions, CES1 was overexpressed in KEL FIB cells, which were then co-cultured with M0 macrophages. Following co-culture, KEL FIB cells were subjected to WB analysis. The results showed that after CES1 overexpression, the pSTAT5 level in KEL FIB cells decreased significantly, whereas total STAT5 expression did not change markedly (Fig. 6A and B). This suggests that CES1 may affect the JAK/STAT signaling cascade by blocking the activation of STAT5. Further WB analysis showed that CES1 overexpression significantly

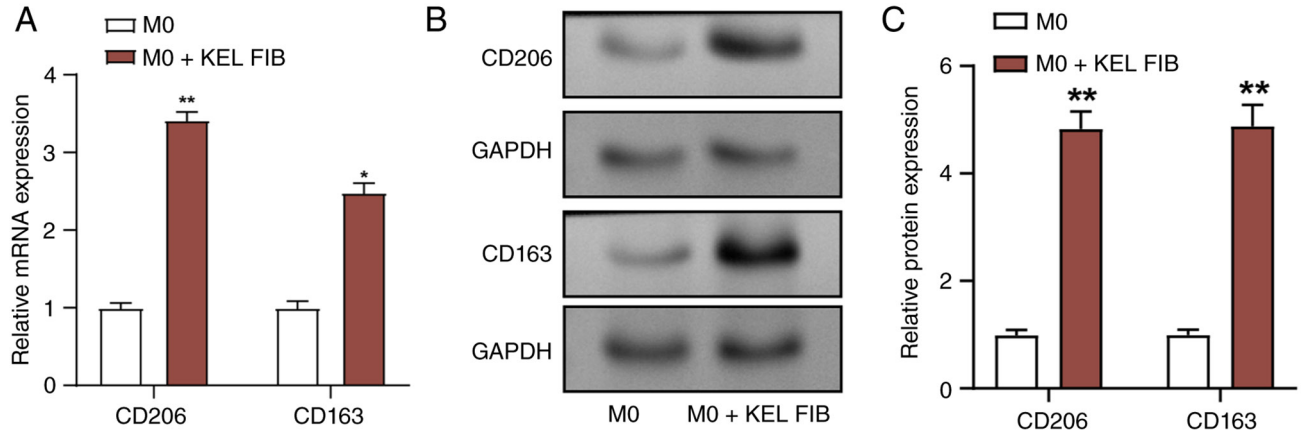


Figure 4. Effects of KEL FIB co-culture on CD206 and CD163 expression in M0 macrophages. (A) Reverse transcription-quantitative PCR analysis measuring the expression levels of M2 macrophage markers (CD206 and CD163) in M0 macrophages or M0 macrophages co-cultured with KEL FIB cells. Statistical analysis was performed using unpaired Student's t-test. (B) Western blot analysis showing the protein expression levels of the M2 macrophage markers CD206 and CD163 in M0 macrophages or in macrophages co-cultured with KEL FIB cells. (C) Corresponding semi-quantification of band intensities is presented in bar graphs. Statistical analysis was performed using unpaired Student's t-test. Data are presented as the mean ± SD (n=3). *P<0.05 and **P<0.01 vs. M0 group.

reduced the levels of multiple fibrosis markers in KEL FIB cells, such as collagen III, collagen I, TGF-β, vimentin, α-SMA and fibronectin (Fig. 6C and D). Immunofluorescence analysis confirmed these findings, showing that after CES1 overexpression, the α-SMA fluorescence intensity was notably reduced in CES1-overexpressing KEL FIB cells co-cultured with M0 macrophages, indicating that this fibrosis marker was downregulated (Fig. 6E). These results suggest that CES1 overexpression is associated with reduced JAK/STAT signaling and lower fibrosis marker expression in keloid fibroblasts.

CES1 is associated with attenuated M2-like macrophage polarization possibly by regulating the JAK/STAT5 signaling pathway in keloid fibroblasts. To investigate the role of CES1 and the JAK/STAT signaling pathway in regulating macrophage polarization under keloid fibroblast-macrophage co-culture conditions, the expression levels of M2 macrophage markers (CD206 and CD163) were evaluated by RT-qPCR and WB analyses in M0 macrophages co-cultured with CES1-overexpressing KEL FIB cells. The results showed that CES1 overexpression in KEL FIB cells suppressed CD206 and CD163 expression in co-cultured M0 macrophages compared with that in controls (Fig. 7A-D). Subsequent WB analysis examined the impact of CES1 knockdown and STAT5 inhibitor (AC-4-130) on pSTAT5 and STAT5 expression levels in KEL FIB cells after co-culture with M0 macrophages. The results revealed that CES1 knockdown in KEL FIB cells led to an increase in pSTAT5 levels, while total STAT5 expression remained unchanged. Notably, the addition of AC-4-130 reversed the increase of pSTAT5 in CES1-knockdown KEL FIB cells, with STAT5 levels again showing no marked change (Fig. 7E and F). Furthermore, RT-qPCR and WB analyses demonstrated that CES1 knockdown promoted CD206 and CD163 expression in co-cultured M0 macrophages, an effect reversed by AC-4-130 treatment (Fig. 7G-K). These findings suggest that CES1 may attenuate M2-like macrophage polarization of M0 macrophages by inhibiting the JAK/STAT signaling pathway in keloid fibroblasts.

Polarized M2 macrophages promote fibrotic characteristics in keloid fibroblasts. To measure M2 macrophage marker levels, RT-qPCR and WB analyses were performed on M0 and M2 macrophages, revealing a notable increase in CD206 and CD163 mRNA and protein levels in M2 macrophages compared with those in M0 macrophages (Fig. 8A-C). Subsequent WB analysis evaluated the expression of fibrosis markers (collagen III, TGF-β, collagen I, vimentin, α-SMA and fibronectin) in CES1-overexpressing KEL FIB cells co-cultured with M2 macrophages. The aforementioned results showed that CES1 overexpression in KEL FIB cells was associated with reduced levels of M0-to-M2-like polarization markers in the co-culture system, accompanied by decreased expression of fibrosis-related factors in KEL FIB cells. By contrast, when pre-polarized M2 macrophages were co-cultured with CES1-overexpressing keloid fibroblasts, M2 cells could have continued to enhance the fibrotic activation of fibroblasts. Consequently, in the presence of exogenous M2 macrophages, fibrosis marker levels did not differ significantly between the CES1-overexpressing and control groups (Fig. 8D and E). These findings suggest that the antifibrotic effect of CES1 potentially relies on inhibiting M0-to-M2 polarization, whereas pre-polarized M2 macrophages can negate this effect. However, this finding is preliminary and requires further validation in subsequent studies.

Discussion

Keloids result from the aberrant proliferation of scar tissue, often attributed to excessive collagen synthesis (30). This condition is frequently accompanied by symptoms such as itching and discomfort, impacting the quality of life of impacted patients. A recent study by Kim and Kim (31) suggested that keloid formation is influenced by multiple factors, including genetic predisposition, dysregulated immune responses and abnormal wound-healing processes. The present study employed differential expression analysis on keloid-related datasets, identifying three overlapping genes: CES1, PLOD3 and SEMA3G. Shao *et al* (32) revealed that knockdown of PLOD3 reduces the

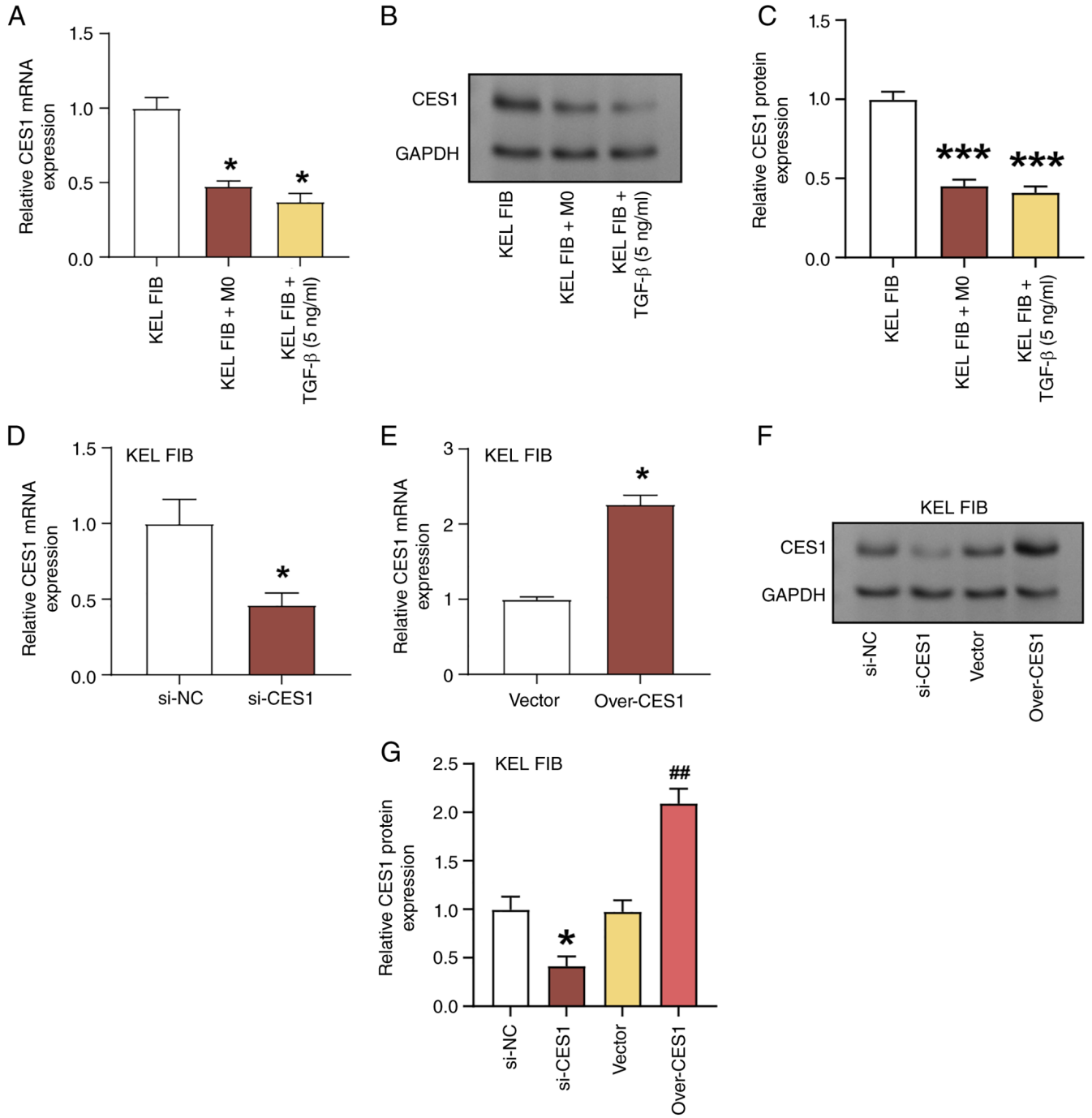


Figure 5. Modulation of CES1 expression in keloid fibroblasts under various conditions. (A) RT-qPCR assessment of CES1 expression in KEL FIB cells across three treatment conditions: KEL FIB cells alone, KEL FIB cells co-cultured with M0 macrophages and KEL FIB cells treated with TGF-β. Statistical analysis was performed using one-way ANOVA followed by Tukey's post hoc test. *P<0.05 vs. KEL FIB group. (B) WB analysis displaying CES1 protein expression and (C) semi-quantification of WB bands in KEL FIB cells under different treatment conditions. Statistical analysis was performed using one-way ANOVA followed by Tukey's post hoc test. ***P<0.001 vs. KEL FIB group. Verification of CES1 (D) knockdown efficiency in KEL FIB cells transfected with si-CES1 or si-NC and (E) overexpression efficiency in KEL FIB cells transfected with the CES1 overexpression vector or control vector, as assessed by RT-qPCR. Statistical analysis was performed using an unpaired Student's t-test. *P<0.05 vs. si-NC or vector. Confirmation of CES1 knockdown and overexpression efficiencies in KEL FIB cells via (F) WB analysis and (G) semi-quantification of protein levels. Statistical analysis was performed using an unpaired Student's t-test. *P<0.05 vs. si-NC group; $^{\#\#}$P<0.01 vs. vector group. Data are presented as the mean ± SD (n=3). si, small interfering; NC, negative control; over, overexpression; CES1, carboxylesterase 1; WB, western blot; RT-qPCR, reverse transcription-quantitative PCR.

expression of lysyl hydroxylase 3 and type I collagen, leading to a decrease in collagen pyridinoline cross-linking products. Conversely, PLOD3 overexpression increases lysyl hydroxylase 3 and collagen I expression, suggesting that PLOD3 promotes collagen cross-linking and the fibrotic process. Luo *et al* (33) demonstrated that SEMA3G secreted by endothelial cells markedly affects the fibrotic process in diabetic conditions by promoting the migration and proliferation of human aortic smooth muscle cells. Given the limited research on the role of CES1 in fibrosis and keloids, the present study aimed to investigate the fundamental mechanisms of CES1 in keloid fibroblasts.

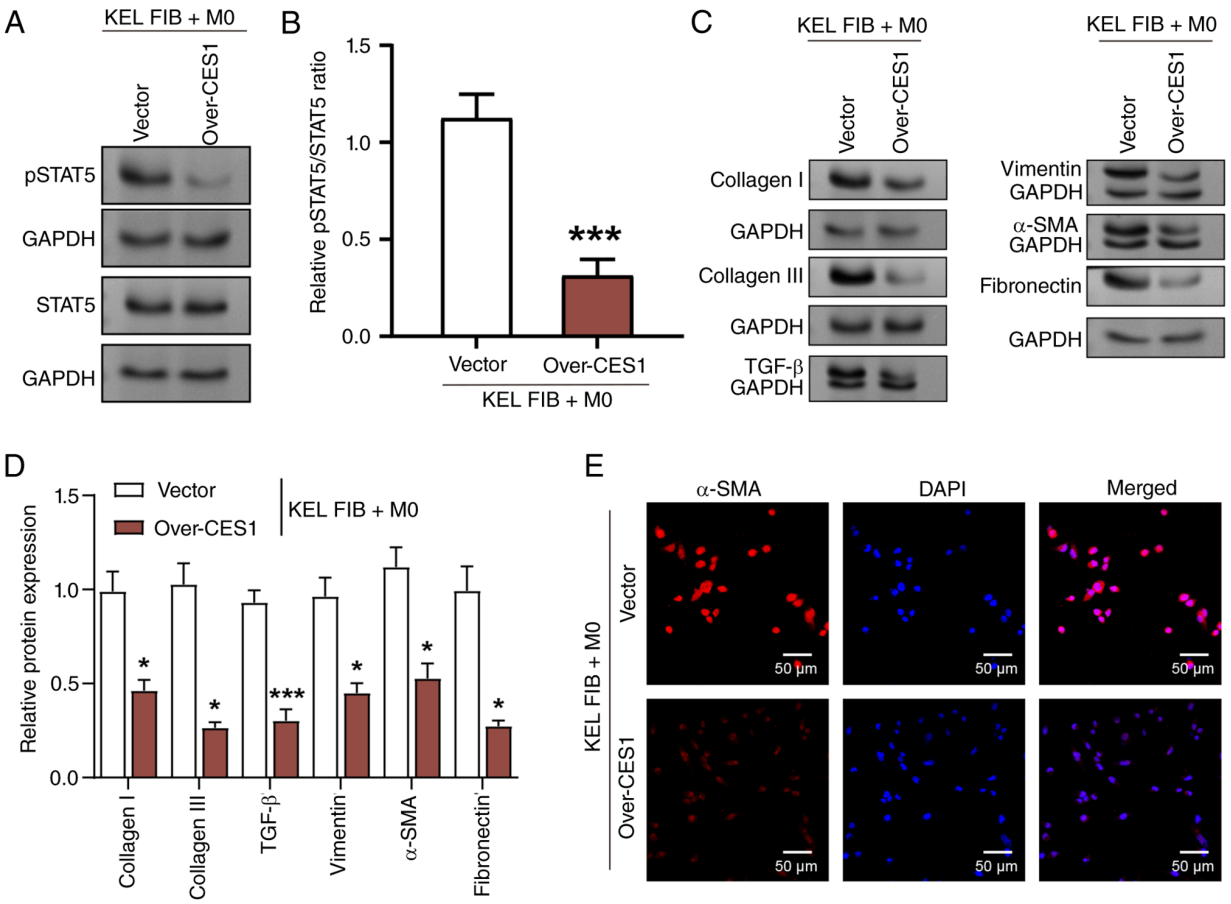


Figure 6. Effects of CES1 overexpression on STAT5 activation and fibrosis-related markers in KEL FIB cells co-cultured with M0 macrophages. (A) Representative western blot images showing pSTAT5 and total STAT5 expression in KEL FIB cells co-cultured with M0 macrophages following CES1 overexpression. (B) Quantification of pSTAT5 relative to total STAT5 in the groups shown in (A) Statistical analysis was performed using unpaired Student's t-test. (C) Representative western blot images showing the expression of fibrosis-related proteins, including collagen I, collagen III, TGF-β, Vimentin, α-SMA and fibronectin, in CES1-overexpressing KEL FIB cells co-cultured with M0 macrophages. (D) Quantification of the fibrosis-related proteins shown in (C). Statistical analysis was performed using unpaired Student's t-test. (E) Immunofluorescence analysis of α-SMA fluorescence intensity in CES1-overexpressing KEL FIB cells co-cultured with M0 macrophages. Data are presented as the mean ± SD (n=3). *P<0.05 and ***P<0.001 vs. vector group. Scale bar, 50 μm. CES1, carboxylesterase 1; WB, western blot; over, overexpression; α-SMA, α-smooth muscle actin; p, phosphorylated.

TGF-β promotes ECM accumulation by enhancing collagen synthesis and inhibiting MMP activity (34). Additionally, multiple therapeutic strategies to inhibit TGF-β activity have been evaluated (35,36). The present study found that co-culturing M0 macrophages with KEL FIB cells markedly enhanced the proliferation of keloid fibroblasts and macrophages and reduced apoptosis. These findings align with the trend observed during the treatment of KEL FIB cells with TGF-β. Xu *et al* (37) reviewed the involvement of macrophages in keloid formation, highlighting the polarization of macrophages in pathological scar development. It was noted that an early increase in M2 cells is associated with susceptibility to abnormal scarring. Furthermore, a decrease in M1 cells and delayed M2 cell polarization contribute to the formation of pathological scars. Lv *et al* (38) also found that the total numbers of polarized M2 macrophages and macrophages in the peripheral blood and local skin of patients with keloids increased markedly, suggesting that macrophage polarization may be associated with keloid formation.

Fibrosis markers, including collagen I, TGF-β, collagen III, vimentin, α-SMA and fibronectin, are widely considered as key mediators of the pathological processes underlying keloid and hypertrophic scar formation (39,40). To further investigate the effects of macrophages on fibroblast-mediated fibrotic phenotypes, the present study evaluated the levels of various fibrosis markers. By detecting the levels of collagen I, collagen III, TGF-β, vimentin, fibronectin and α-SMA, it was found that the expression levels of fibrosis markers in keloid fibroblasts were notably increased after co-culture with M0 macrophages, confirming that macrophages can induce the fibrotic transformation of keloid fibroblasts.

Previous studies have focused on the regulatory effects of fibrosis markers and their signaling pathways, exploring possible molecular mechanisms underlying fibrosis. Kim *et al* (41) showed that zinc-α-2-glycoprotein-derived peptides effectively reduce the levels of collagen III and collagen I in fibroblasts by inhibiting TGF-β and pSmad2/3 signaling pathways, while also reducing cell proliferation during wound healing. Liu *et al* (42) emphasized that asporin is strongly expressed in keloids, disrupts the response of fibroblasts to mechanical stimulation and prevents their differentiation into mature α-SMA^{+} myofibroblasts. This interference leads to impaired remodeling of the collagen matrix and abnormal proliferation. Cui *et al* (43) found that extra

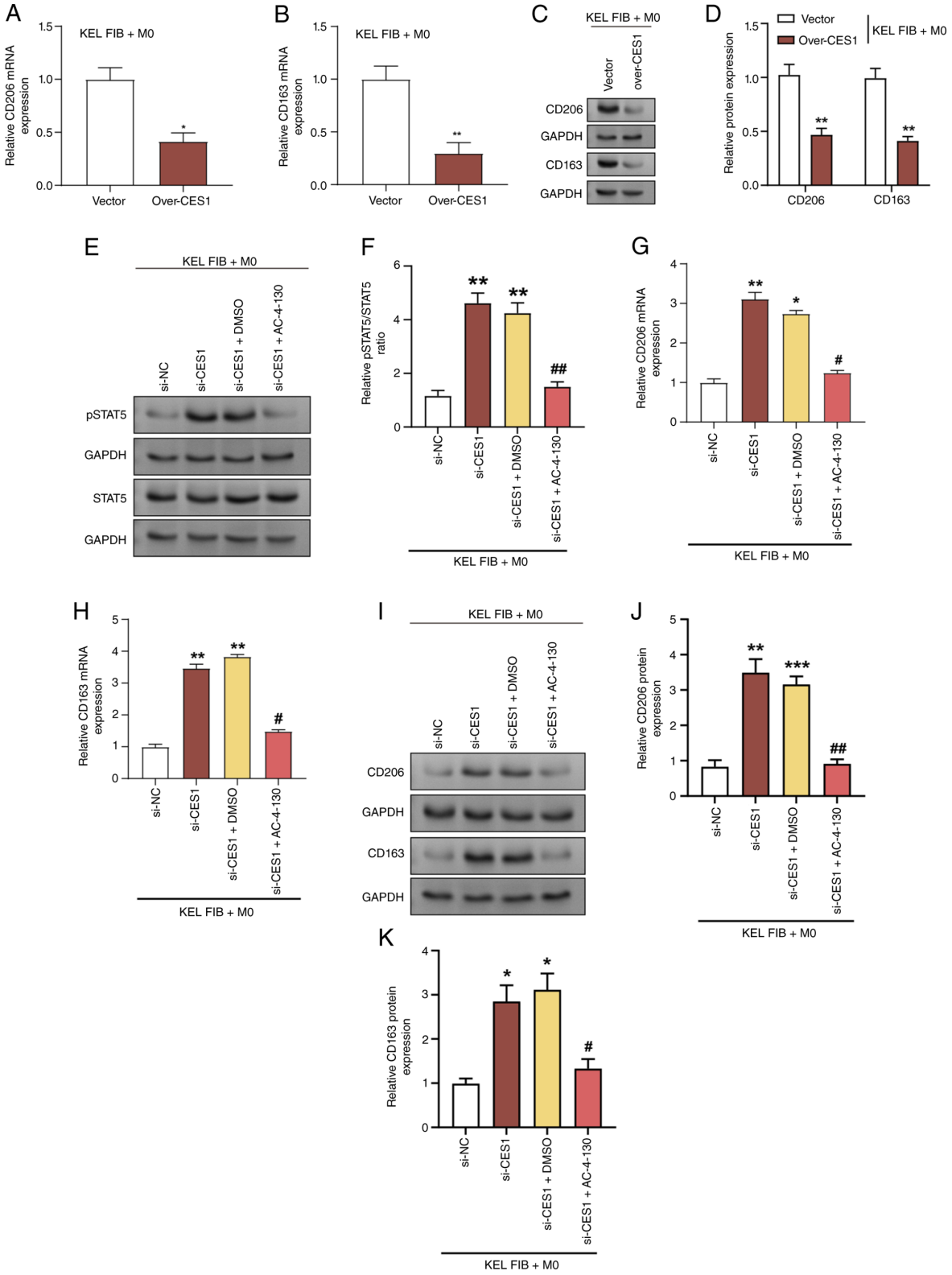


Figure 7. CES1 inhibits M2 macrophage polarization by modulating the JAK/STAT5 signaling pathway in keloid fibroblasts. (A) RT-qPCR analysis of CD206 mRNA expression in M0 macrophages co-cultured with vector- or CES1-overexpressing KEL FIB cells. (B) RT-qPCR analysis of CD163 mRNA expression in M0 macrophages co-cultured with vector- or CES1-overexpressing KEL FIB cells. (C) Representative western blot images and (D) quantification of CD206 and CD163 protein expression in M0 macrophages co-cultured with vector- or CES1-overexpressing KEL FIB cells. Statistical comparisons in (A), (B) and (D) were performed using unpaired Student's t-test. (E) Representative western blot images and (F) quantification of pSTAT5 and total STAT5 levels in KEL FIB cells co-cultured with M0 macrophages under the si-NC, si-CES1, si-CES1 + DMSO and si-CES1 + AC-4-130 conditions. (G) RT-qPCR analysis of CD206 mRNA expression in co-cultured M0 macrophages under the indicated treatment conditions. (H) RT-qPCR analysis of CD163 mRNA expression in co-cultured M0 macrophages under the indicated treatment conditions. (I) Representative western blot images and quantification of (J) CD206 and (K) CD163 protein expression in co-cultured M0 macrophages under the indicated treatment conditions. Statistical comparisons in (F-H), (J) and (K) were performed using one-way ANOVA followed by Tukey's post hoc test. Data are presented as the mean ± SD (n=3). *P<0.05, **P<0.01 and ***P<0.001 vs. vector group or si-NC group; $^{\#}$P<0.05 and $^{\#\#}$P<0.01 vs. si-CES1 + DMSO group. si, small interfering; NC, negative control; over, overexpression; CES1, carboxylesterase 1; WB, western blot; RT-qPCR, reverse transcription-quantitative PCR; p, phosphorylated.

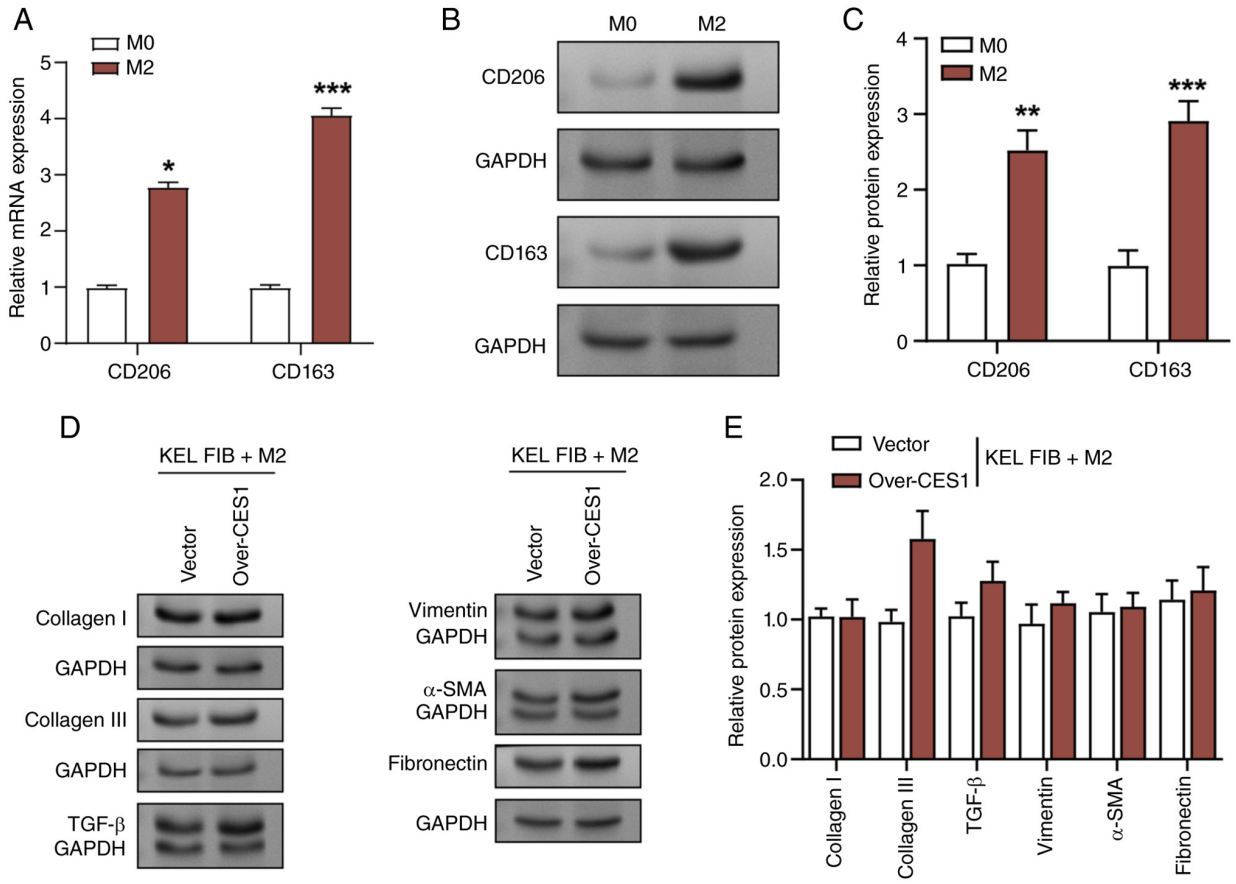


Figure 8. Fibrotic induction by polarized M2 macrophages in keloid fibroblasts. (A) Relative mRNA expression levels of CD206 and CD163 in M0 and M2 macrophages were determined by reverse transcription-quantitative PCR. Statistical analysis was performed using unpaired Student's t-test. (B) WB analysis and (C) semi-quantification of CD206 and CD163 protein expression levels in M0 and M2 macrophages. Statistical analysis was performed using unpaired Student's t-test. (D) WB analysis and (E) semi-quantification of fibrosis-related protein levels (collagen I, collagen III, TGF-β, vimentin, α-SMA and fibronectin) in KEL FIB cells transfected with over-CES1 or vector control, and co-cultured with polarized M2 macrophages. Statistical analysis was performed using unpaired Student's t-test. Data are presented as the mean ± SD (n=3). *P<0.05, **P<0.01 and ***P<0.001 vs. M0 group. CES1, carboxylesterase 1; WB, western blot; over, overexpression; α-SMA, α-smooth muscle actin.

domain B (EDB) of fibronectin is highly expressed in keloid tissue. The study showed that silencing EDB notably inhibited TGF-β1-induced proliferation and collagen deposition in keloid fibroblasts. Furthermore, it was demonstrated that EDB is necessary in keloid formation by activating TGF-β1/Smad, ERK and AKT signaling pathways.

CD206 is a widely recognized marker of M2 macrophages, which are important for anti-inflammatory processes, tissue repair and immune regulation (44). Similarly, CD163 is mainly expressed in M2 macrophages and helps clear hemoglobin-haptoglobin complexes, thereby reducing oxidative stress and promoting tissue remodeling (45). The expression of CD206 and CD163 is closely associated with macrophage polarization toward an M2 phenotype, which is characterized by anti-inflammatory and pro-repair functions. Previous studies have also highlighted the role of CD206 and CD163 in keloid formation. Wang and Hu (46) found that the tRNA-derived fragment tsRNA-14783 promotes keloid development by increasing M2 macrophage markers, including TGF-β, IL-10 and CD206, thereby enhancing tissue fibrosis and ECM deposition. In another study, Lee *et al* (47) demonstrated that cryotherapy upregulated $CD163^{+}$ M2 macrophages and MMP-9, suggesting that the recruitment of M2 macrophages serves an important role in tissue remodeling during keloid treatment. This apparent discrepancy may reflect the context-dependent role of M2 macrophages, which can promote fibrosis during keloid formation but facilitate matrix remodeling during treatment. The present experimental results further supported the key role of macrophage polarization in the pathogenesis of keloids. KEL FIB cells were shown to induce the polarization of M0 macrophages to the M2-like phenotype, as evidenced by the notable upregulation of CD206 and CD163 at both the mRNA and protein levels. These results highlight the interaction between fibroblasts and macrophages in keloid progression and suggest that targeting macrophage polarization may represent a new strategy for keloid treatment.

A previous study showed that CES1 is a key component in the hydrolysis pathway of anti-inflammatory prostaglandin D2-glycerol ester (PGD2-G) in THP-1 monocytes and that inhibition of CES1 activity with small-molecule inhibitors enhances the anti-inflammatory effects of PGD2-G (48). These findings suggest that CES1 may influence fibrotic responses by modulating macrophage inflammatory and polarization states, providing a potential link between CES1 activity and keloid fibrosis. The JAK/STAT signaling pathway, a key regulatory mechanism involved in macrophage polarization

and fibroblast activation, has garnered attention regarding its impact on keloid formation. Chao *et al* (49) found increased activation of the M2 macrophage subtype in scar tissue, with elevated levels of pSTAT6 associated with keloid fibrosis. The ectopic expression of IL-13 receptor subunit α2 in keloid fibroblasts was shown to inhibit STAT6 activation and cell proliferation. Zhou *et al* (50) showed that AG490, a selective inhibitor of the JAK2/STAT3 pathway, effectively suppresses the proliferation of human keloid fibroblasts by inducing apoptosis and cell cycle arrest. AC-4-130 is a small-molecule compound that specifically inhibits the STAT5 signaling pathway, reducing STAT5 phosphorylation and transcriptional activity in cells. The present study demonstrated that CES1 is downregulated in keloid fibroblasts and may be associated with mitigating fibrosis, potentially through inhibition of the JAK/STAT signaling pathway. Overexpression of CES1 could reduce the levels of pSTAT5 and fibrosis markers, such as collagen I and III, as well as TGF-β, and was associated with the inhibition of M2-like macrophage polarization. However, polarized M2 macrophages may directly promote fibrosis in keloid fibroblasts, counteracting the inhibitory effects of CES1 overexpression. From a therapeutic perspective, this finding suggests that CES1-based interventions may be more suitable for early prevention rather than reversing established fibrosis, and underscores the important role of M2 macrophages in scar formation.

Several limitations of the present study should be noted. First, all experiments were performed using commercial cell lines rather than primary keloid fibroblasts or primary macrophages, which may not fully capture the native cellular context. Second, the co-culture system lacked cell-type-specific genetic manipulation, limiting the precise attribution of signaling events. Third, direct causal evidence remains insufficient, and additional rescue and targeted validation experiments are required. Fourth, no clinical keloid specimens or *in vivo* models were included. These limitations should be addressed in future studies incorporating clinical tissues and animal experiments to enhance the robustness and generalizability of the present findings.

In conclusion, the present investigation provided preliminary evidence for a potential role of CES1 in modulating fibrosis and M2-like macrophage polarization in the etiology of keloids. The results demonstrated that CES1 expression is reduced in keloid fibroblasts and that its overexpression is associated with the inhibition of the JAK/STAT signaling pathway, thereby reducing fibrotic markers and suppressing M2 polarization. Furthermore, the findings indicated that M0 macrophages may contribute to keloid fibroblast proliferation and fibrotic changes, accompanied by M2-like polarization, underscoring the intricate interplay between macrophages and fibroblasts during keloid formation. These findings suggest that CES1 and the macrophage-fibroblast axis may represent a promising research direction for keloid fibrosis, and future studies incorporating *in vivo* models and clinical specimens are warranted to further validate their potential as therapeutic targets.

Acknowledgements

Not applicable.

Funding

The present study was funded by the National Natural Science Foundation of China (grant no. 82100983).

Availability of data and materials

The data generated in the present study may be requested from the corresponding author.

Authors' contributions

QJ, YH and YC were involved in the conception and design of the research. QJ and YH acquired data. QJ, YH, JQ, XF, SX and HS performed analysis and interpretation of data. JQ, XF, SX and HS performed the statistical analysis. QJ and YH drafted the manuscript. YC revised the manuscript for important intellectual content. QJ and YH confirm the authenticity of all the raw data. All authors have read and approved the final version of the manuscript.

Ethics approval and consent to participate

Not applicable.

Patient consent for publication

Not applicable.

Competing interests

The authors declare that they have no competing interests.

References

1. Férnandez-Guarino M, Naharro-Rodriguez J and Bacci S: Disturbances in the skin homeostasis: Wound healing, an undefined process. Cosmetics 11: 90, 2024.
2. Sitaniya S, Subramani D, Jadhav A, Sharma YK, Deora MS and Gupta A: Quality-of-life of people with keloids and its correlation with clinical severity and demographic profiles. Wound Repair Regen 30: 409-416, 2022.
3. Gwen Farm HJ, Dwivedi A, Ranjbar D, Chai B, Le M and Liu C: The association between race/ethnicity and keloid formation: A network meta-analysis. Plast Surg (Oakv): 22925503261470272, 2026 doi: 10.1177/22925503261470272 (Epub ahead of print).
4. Walsh LA, Wu E, Pontes D, Kwan KR, Poondru S, Miller CH and Kundu RV: Keloid treatments: an evidence-based systematic review of recent advances. Syst Rev 12: 42, 2023.
5. Ekstein SF, Wyles SP, Moran SL and Meves A: Keloids: A review of therapeutic management. Int J Dermatol 60: 661-671, 2021.
6. Feng F, Liu M, Pan L, Wu J, Wang C, Yang L, Liu W, Xu W and Lei M: Biomechanical regulatory factors and therapeutic targets in keloid fibrosis. Front Pharmacol 13: 906212, 2022.
7. Hong YK, Chang YH, Lin YC, Chen B, Guevara BEK and Hsu CK: Inflammation in wound healing and pathological scarring. Adv Wound Care (New Rochelle) 12: 288-300, 2023.
8. Zhang M, Chen H, Qian H and Wang C: Characterization of the skin keloid microenvironment. Cell Commun Signal 21: 207, 2023.
9. Rodríguez-Morales P and Franklin RA: Macrophage phenotypes and functions: Resolving inflammation and restoring homeostasis. Trends Immunol 44: 986-998, 2023.
10. Yang H, Cheng H, Dai R, Shang L, Zhang X and Wen H: Macrophage polarization in tissue fibrosis. PeerJ 11: e16092, 2023.
11. Seoudy WM, Mohy El Dien SM, Abdel Reheem TA, Elfangary MM and Erfan MA: Macrophages of the M1 and M2 types play a role in keloids pathogenesis. Int Wound J 20: 38-45, 2023.

12. Dirand Z, Maraux M, Tissot M, Chatelain B, Supp D, Viennet C, Perruche S and Rolin G: Macrophage phenotype is determinant for fibrosis development in keloid disease. Matrix Biology 128: 79-92, 2024.
13. Hu Q, Bian Q, Rong D, Wang L, Song J, Huang HS, Zeng J, Mei J and Wang PY: JAK/STAT pathway: Extracellular signals, diseases, immunity, and therapeutic regimens. Front Bioeng Biotechnol 11: 1110765, 2023.
14. Xue C, Yao Q, Gu X, Shi Q, Yuan X, Chu Q, Bao Z, Lu J and Li L: Evolving cognition of the JAK-STAT signaling pathway: Autoimmune disorders and cancer. Signal Transduct Target Ther 8: 204, 2023.
15. Liu J, Wang F and Luo F: The role of JAK/STAT pathway in fibrotic diseases: Molecular and cellular mechanisms. Biomolecules 13: 119, 2023.
16. Chen JY, Feng QL, Pan HH, Zhu DH, He RL, Deng CC and Yang B: An open-label, uncontrolled, single-arm clinical trial of tofacitinib, an oral JAK1 and JAK3 kinase inhibitor, in Chinese patients with keloid. Dermatology 239: 818-827, 2023.
17. Lopez-Bergami P and Barbero G: The emerging role of Wnt5a in the promotion of a pro-inflammatory and immunosuppressive tumor microenvironment. Cancer Metastasis Rev 39: 933-952, 2020.
18. Huang JG, Ren JX, Chen Y, Tian MF, Zhou L, Wen J, Song XS, Wu YL, Yang QH, Jiang PR, *et al*: M2 macrophages mediate fibrotic scar formation in the early stages after cerebral ischemia in rats. Neural Regen Res 18: 2208-2218, 2023.
19. Widowati W, Sabrina AHN, Sutendi AF, Zahiroh FH, Wargasetia TL, Nainggolan IM, Rismani E and Vosough M: M2 macrophages-based immunotherapy: A new therapeutic approach in liver fibrosis. Adv Pharm Bull 15: 314-325, 2025.
20. Jiang C, Liu C, Yao XI, Su J, Lu W, Wei Z and Xie Y: CES1 is associated with cisplatin resistance and poor prognosis of head and neck squamous cell carcinoma. Oncol Res 32: 1935, 2024.
21. Li G, Li X, Mahmud I, Ysaguirre J, Fekry B, Wang S, Wei B, Eckel-Mahan KL, Lorenzi PL, Lehner R and Sun K: Interfering with lipid metabolism through targeting CES1 sensitizes hepatocellular carcinoma for chemotherapy. JCI Insight 8: e163624, 2023.
22. Fuentes-Duculan J, Bonifacio KM, Suárez-Fariñas M, Kunjravia N, Garcet S, Cruz T, Wang CQF, Xu H, Gilleadeau P, Sullivan-Whalen M, *et al*: Aberrant connective tissue differentiation towards cartilage and bone underlies human keloids in African Americans. Exp Dermatol 26: 721-727, 2017.
23. Matsumoto NM, Aoki M, Okubo Y, Kuwahara K, Eura S, Dohi T, Akaishi S and Ogawa R: Gene expression profile of isolated dermal vascular endothelial cells in keloids. Front Cell Dev Biol 8: 658, 2020.
24. Hickman E, Smyth T, Cobos-Uribe C, Immormino R, Rebuli ME, Moran T, Alexis NE and Jaspers I: Expanded characterization of in vitro polarized M0, M1, and M2 human monocyte-derived macrophages: Bioenergetic and secreted mediator profiles. PLoS One 18: e0279037, 2023.
25. Adams G: A beginner's guide to RT-PCR, qPCR and RT-qPCR. Biochemist 42: 48-53, 2020.
26. Prins KW and Goncharova EA: CES1 links lipid dysregulation and endothelial pathology in pulmonary arterial hypertension. Am J Respir Crit Care Med 212: 1195-1197, 2026.
27. Sun K: CES1/Ces1d at the crossroads of intracellular lipolysis, lipid signaling, and metabolic remodeling. Trends Open, 2026 doi: 10.1016/j.treopn.2026.07.015.
28. Antar SA, Ashour NA, Marawan ME and Al-Karmalawy AA: Fibrosis: Types, effects, markers, mechanisms for disease progression, and its relation with oxidative stress, immunity, and inflammation. Int J Mol Sci 24: 4004, 2023.
29. Ni D, Zhou H, Wang P, Xu F and Li C: Visualizing macrophage phenotypes and polarization in diseases: From biomarkers to Molecular Probes. Phenomics 3: 613-638, 2023.
30. Limandjaja GC, Niessen FB, Scheper RJ and Gibbs S: Hypertrophic scars and keloids: Overview of the evidence and practical guide for differentiating between these abnormal scars. Exp Dermatol 30: 146-161, 2021.
31. Kim HJ and Kim YH: Comprehensive insights into keloid pathogenesis and advanced therapeutic strategies. Int J Mol Sci 25: 8776, 2024.
32. Shao S, Fang H, Duan L, Ye X, Rao S, Han J, Li Y, Yuan G, Liu W and Zhang X: Lysyl hydroxylase 3 increases collagen deposition and promotes pulmonary fibrosis by activating TGFβ1/Smad3 and Wnt/β-catenin pathways. Arch Med Sci 16: 436-445, 2020.
33. Luo XY, Fu X, Liu F, Luo JY and Chen AF: Sema3G activates YAP and promotes VSMCs proliferation and migration via Nrp2/PlexinA1. Cell Signal 105: 110613, 2023.
34. Chen F, Lyu L, Xing C, Chen Y, Hu S, Wang M and Ai Z: The pivotal role of TGF-β/Smad pathway in fibrosis pathogenesis and treatment. Front Oncol 15: 1649179, 2025.
35. Zhu W, Cui Y, Qiu J, Zhang X, Gao Y, Shang Z and Huang L: Exploring the therapeutic potential of TGF-β inhibitors for liver fibrosis: Targeting multiple signaling pathways. J Clin Transl Hepatol 13: 588, 2025.
36. Adhikari S, Singh V, Nandi S, Ghosal M, Raj NS, Khanna J, Bhattacharya A, Kabiraj A, Mondal A, Vasudevan M, *et al*: UBR7 in concert with EZH2 inhibits the TGF-β signaling leading to extracellular matrix remodeling. Cell Rep 43: 114394, 2024.
37. Xu X, Gu S, Huang X, Ren J, Gu Y, Wei C, Lian X, Li H, Gao Y, Jin R, *et al*: The role of macrophages in the formation of hypertrophic scars and keloids. Burns Trauma 8: tkaa006, 2020.
38. Lv X, He Z, Yang M, Wang L and Fu S: Analysis of subsets and localization of macrophages in skin lesions and peripheral blood of patients with keloids. Heliyon 10: e24034, 2024.
39. Čoma M, Fröhlichová L, Urban L, Zajíček R, Urban T, Szabo P, Novák Š, Fetissov V, Dvořánková B, Smetana K Jr and Gál P: Molecular changes underlying hypertrophic scarring following burns involve specific deregulations at all wound healing stages (inflammation, proliferation and maturation). Int J Mol Sci 22: 897, 2021.
40. Macarak EJ, Wermuth PJ, Rosenbloom J and Uitto J: Keloid disorder: Fibroblast differentiation and gene expression profile in fibrotic skin diseases. Exp Dermatol 30: 132-145, 2021.
41. Kim SH, Oh JM, Roh H, Lee KW, Lee JH and Lee WJ: Zinc-Alpha-2-glycoprotein peptide downregulates type I and III collagen expression via suppression of TGF-β and p-Smad 2/3 pathway in keloid fibroblasts and rat incisional model. Tissue Eng Regen Med 21: 1079-1092, 2024.
42. Liu L, Yu H, Long Y, You Z, Ogawa R, Du Y and Huang C: Asporin inhibits collagen matrix-mediated intercellular mechanocommunications between fibroblasts during keloid progression. FASEB J 35: e21705, 2021.
43. Cui J, Li Z, Jin C and Jin Z: Knockdown of fibronectin extra domain B suppresses TGF-β1-mediated cell proliferation and collagen deposition in keloid fibroblasts via AKT/ERK signaling pathway. Biochem Biophys Res Commun 526: 1131-1137, 2020.
44. Li H, Miao YQ, Suo LP, Wang X, Mao YQ, Zhang XH, Zhou N, Tian JR, Yu XY, Wang TX, *et al*: CD206 modulates the role of M2 macrophages in the origin of metastatic tumors. J Cancer 15: 1462-1486, 2024.
45. Ferreira DW, Ulecia-Morón C, Alvarado-Vázquez PA, Cunnane K, Moracho-Vilriales C, Grosick RL, Cunha TM and Romero-Sandoval EA: CD163 overexpression using a macrophage-directed gene therapy approach improves wound healing in ex vivo and in vivo human skin models. Immunobiology 225: 151862, 2020.
46. Wang X and Hu Z: tRNA derived fragment tsRNA-14783 promotes M2 polarization of macrophages in keloid. Biochem Biophys Res Commun 636: 119-127, 2022.
47. Lee YI, Kim SM, Jihee K, Jemin K, Song SY, Lee WJ and Lee JH: Tissue-remodelling M2 macrophages recruits matrix metallo-proteinase-9 for cryotherapy-induced fibrotic resolution during keloid treatment. Acta Derm Venereol 100: adv00306, 2020.
48. Scheaffer HL, Borazjani A, Szafran BN and Ross MK: Inactivation of CES1 blocks prostaglandin D2 glyceryl ester catabolism in monocytes/Macrophages and enhances its anti-inflammatory effects, whereas the Pro-inflammatory effects of prostaglandin E2 Glyceryl ester are attenuated. ACS Omega 5: 29177-29188, 2020.
49. Chao H, Zheng L, Hsu P, He J, Wu R, Xu S, Zeng R, Zhou Y, Ma H, Liu H and Tang Q: IL-13RA2 downregulation in fibroblasts promotes keloid fibrosis via JAK/STAT6 activation. JCI insight 8: e157091, 2023.
50. Zhou Y, Sun Y, Hou W, Ma L, Tao Y, Li D, Xu C, Bao J and Fan W: The JAK2/STAT3 pathway inhibitor, AG490, suppresses the abnormal behavior of keloid fibroblasts *in vitro*. Int J Mol Med 46: 191-200, 2020.

Copyright © 2026 Jin et al. This work is licensed under a Creative Commons Attribution-NonCommercial-NoDerivatives 4.0 International (CC BY-NC-ND 4.0) License.